s- and p-Wave π-π Phase Shifts at Low Energies*

BRYAN F. GORE†
University of Michigan, Ann Arbor, Michigan 48104
(Received 10 January 1969)

The Lorentz-invariant π-π scattering amplitude is investigated on the basis of the analyticity and unitarity of the S matrix. The assumptions of elastic unitarity and approximate crossing symmetry allow the calculation of subtracted dispersion integrals for s and p partial waves. Of the seven parameters introduced, five are fixed by derivative conditions to third order from crossing symmetry, and the others by the requirement that the p-wave solution exhibit a resonance of mass 750 MeV and width 110 MeV. The computations were iterated by computer. Five different parametrizations are investigated; nine solutions are found, belonging to three parametrizations. Six of the solutions belong to one parametrization; the others are similar. Various model calculations reported in the literature yield solutions similar to ours, but no model has produced our complete spectrum. A "best" solution is selected on the basis of self-consistency and lack of nearby physical-sheet poles of the scattering amplitude. It is characterized by s-wave phase shifts dropping from threshold. The phase-shift decreases at the ρ-meson mass are $(72\pm3)°$ for $I=0$ and $(41\pm4)°$ for $I=2$. The p-wave phase shift is similar to that of a Breit-Wigner resonance, but does not approach 180° as rapidly. The scattering lengths are $\mu a_0{}^0=-0.69\pm0.04$, $\mu a_0{}^2=-0.37\pm0.03$, and $\mu^3 a_1{}^1=0.028$.

I. INTRODUCTION

THE dominant feature of low-energy π-π scattering is the ρ meson, a p-wave isospin-1 resonance. The persistent forward-backward asymmetry of the scattering has led to various conjectures about the phase shifts of the s waves which interfere with the p wave. In this investigation, sets of s- and p-wave phase shifts are determined for energies from threshold to above the ρ mass. The inverse-amplitude formulation of S-matrix theory is used, with elastic unitarity giving the singularities of the s- and p-wave inverse partial-wave amplitudes above threshold. Subtracted dispersion relations introduce parameters into the calculation, which are fixed by the application of crossing symmetry at the centroid of the Mandelstam triangle, plus two conditions based upon the existence of the ρ meson. Calculations are iterated by computer. Because all parameters are evaluated, the results are not dependent on coupling constants, except through the measured mass and width of the ρ.

The inverse-amplitude approach to low-energy π-π scattering has had some success in explaining this phenomenon. Moffat[1] was able to produce a p-wave resonance while neglecting s waves in a one-parameter theory. Later, Bransden and Moffat[2] included s waves to make the calculation more complete. This calculation, also in terms of one parameter, retained the p-wave resonance. More recently Kang,[3,4] also in a one-parameter calculation, has produced this resonant behavior. In all but the first of these calculations, information was also gathered on the s-wave amplitudes for isospin 0 and 2. However, because of the poor agreement of the p-wave results with the measured mass and width of the ρ meson, these results must be regarded as questionable. In this investigation, the existence of the ρ meson is incorporated into the formulation. In particular, the ρ mass and width are used in the determination of parameters in the direct channel. (It should be noted that this calculation differs from the bootstraps, where ρ-mass and -width input in the crossed channel generates a resonance in the direct channel.)

In writing dispersion relations for the inverse partial-wave amplitudes we assume that they have no poles within the closed contour of integration. The possibility of poles in their real parts on the real axis is investigated, however. Five different parametrizations are considered, four of which allow single poles on the real axis in one or more of the inverse partial-wave amplitudes.

II. GENERAL FORMULATION

We work with the Lorentz-invariant scattering amplitude related to the S matrix by

$$S_{fi}=\delta_{fi}+4\pi i(2\pi)^4\delta^4(p_f-p_i)\frac{A(s,t,u)}{(w_1w_2w_3w_4)^{1/2}}, \quad (1)$$

where the w's are the pion energies, and s, t, and u are the usual variables formed from the pion four-momenta. In terms of the square of the center-of-mass momentum ν and the scattering angle θ (units $\hbar=c=m_\pi=1$), $s=4(\nu+1)$, $t=-2\nu(1-\cos\theta)$, and $u=4-s-t$.

The scattering amplitude is separated into isospin amplitudes and analyzed into partial waves. The unitarity of the S matrix allows us to write, for physical energies ($\nu>0$),

$$A_l{}^I(\nu)^{-1}=[\nu/(\nu+1)]^{1/2}(\cot\delta_l{}^I-i). \quad (2)$$

The phase shifts are real for elastic scattering, and

* Financial support provided primarily by the U. S. Atomic Energy Commission. A Faculty Research Fellowship at the University of Idaho is also gratefully acknowledged.

† Present address: Central Washington State College, Ellensburg, Wash. 98926.

[1] J. W. Moffat, Phys. Rev. **121**, 926 (1961).

[2] B. H. Bransden and J. W. Moffat, Nuovo Cimento **21**, 505 (1961); Phys. Rev. Letters **8**, 145 (1962).

[3] K. Kang, Phys. Rev. **134**, B1324 (1964).

[4] K. Kang, Phys. Rev. **139**, B126 (1965).

become complex at the threshold for inelastic intermediate states, which occurs at $\nu=3$. In this paper they are assumed to be real at all energies; this is the assumption of elastic unitarity.

We choose to write dispersion relations for $F_l^I(\nu)=\nu^l A_l^I(\nu)^{-1}$, since they lack the threshold singularities of $A_l^I(\nu)$; poles and zeros, of course, interchange. If we assume that the amplitude has only those singularities required by unitarity in the direct and crossed channels, $F_l^I(\nu)$ is seen to have branch cuts on the real axis from $\nu=0$ to ∞ and from -1 to $-\infty$. To force convergence of the integrals and to limit their sensitivity to $\mathrm{Im}F_l^I(\nu)$ at large $|\nu|$, we perform $l+1$ subtractions at $\nu=0$ in each integral. Then

$$F_l^I(\nu)=\sum_{k=0}^{l} a_k^I\nu^k+\frac{\nu^{l+1}}{\pi}\int_0^\infty\frac{\mathrm{Im}F_l^I(\nu')d\nu'}{\nu'^{l+1}(\nu'-\nu)}+\frac{\nu^{l+1}}{\pi}\int_{-\infty}^{-1}\frac{\mathrm{Im}F_l^I(\nu')d\nu'}{\nu'^{l+1}(\nu'-\nu)}+\frac{\nu^{l+1}}{2\pi i}\int_{\text{closure as }|\nu'|\to\infty}\frac{F_l^I(\nu')d\nu'}{(\nu'-\nu)\nu'^{l+1}}. \quad (3)$$

The effect of these subtractions is to exchange our ignorance of $\mathrm{Im}F_l^I(\nu)$ at large ν for a polynomial involving unknown parameters. We can evaluate these parameters using crossing symmetry, however, and thus proceed with the calculation.

If we assume that the contribution of the closure integral can be absorbed into the parametrization, for ν with a small positive imaginary part this becomes

$$F_l^I(\nu)=\mathcal{P}_l^I(\nu)+\nu^l f(\nu)+L_l^I(\nu)-i\left[\left(\frac{\nu^{2l+1}}{\nu+1}\right)^{1/2}\theta(\nu)+\frac{\nu^l\,\mathrm{Im}A_l^I(\nu)}{|A_l^I(\nu)|^2}\theta(-\nu-1)\right], \quad (4)$$

where

$$\mathcal{P}_l^I(\nu)=\sum_{k=0}^{l} a_k^I\nu^k+\frac{\nu^{l+1}}{2\pi i}\int_{\text{closure as }|\nu'|\to\infty}\frac{F_l^I(\nu')d\nu'}{\nu'^{l+1}(\nu'-\nu)}, \quad (5)$$

$$f(\nu)=\frac{2}{\pi}\left(\frac{\nu}{\nu+1}\right)^{1/2}\ln(\sqrt{|\nu+1|}+\sqrt{|\nu|})\quad\text{for }\nu>0\text{ or }\nu<-1$$
$$=\frac{2}{\pi}\left(\frac{-\nu}{1+\nu}\right)^{1/2}\tan^{-1}\left(\frac{1+\nu}{-\nu}\right)^{1/2}\quad\text{for }-1<\nu<0, \quad (6)$$

$$L_l^I(\nu)=-\frac{\nu^{l+1}}{\pi}P\int_{-\infty}^{-1}\frac{\mathrm{Im}A_l^I(\nu')d\nu'}{\nu'(\nu'-\nu)|A_l^I(\nu')|^2}, \quad (7)$$

$\theta(\nu)$ is the unit step function at the origin, and P indicates the principal value of the integral. Separate calculations are performed for five different parametrizations.

The contribution to $\mathcal{P}_l^I(\nu)$ from the closure integral depends on our assumption of the behavior of $A_l^I(\nu\to\infty)$. Unitarity indicates that $A_l^I(\nu)$ will be bounded by a constant as $|\nu|\to\infty$. If this constant is not zero, we may neglect the contribution for ν far from the closure. If $A_l^I(\nu)$ approaches zero as ν becomes infinite, the contribution is of higher order in ν than l, and more terms must be added to the polynomial. The parametrizations, which are discussed in Sec. III, are consistent with $A_l^I(\nu\to\infty)$ either approaching a constant or vanishing as $1/\nu$. We do not feel, however, that a choice of parametrization necessarily implies the corresponding assumption of behavior for $A_l^I(\nu\to\infty)$, since it is certain that our equations are not valid for very large ν.

Evaluation of the integral in Eq. (7) is dependent upon knowledge of the integrand. Although unitarity in the direct channel is only useful for $\nu>0$, we may use crossing symmetry to find $\mathrm{Im}A_l^I(\nu<-1)$ from the unitarity cut in the crossed channels. For $\nu<-1$,

$$\mathrm{Im}A_l^I(\nu)=\frac{2}{\nu}\int_0^{-\nu-1}d\nu' P_l\left(1+2\frac{\nu'+1}{\nu}\right)\times\sum_{l'}\chi_{ll'}\sum_{l'}(2l'+1)P_{l'}\left(1+2\frac{\nu+1}{\nu'}\right)\mathrm{Im}A_{l'}^{I'}(\nu'), \quad (8)$$

where χ is the self-inverse crossing matrix

$$\chi=\begin{bmatrix}1/3 & 1 & 5/3\\ 1/3 & 1/2 & -5/6\\ 1/3 & -1/2 & 1/6\end{bmatrix}. \quad (9)$$

When $\mathrm{Re}[A_l^I(\nu)^{-1}]$ are known, Eq. (7) is used with the substitution

$$\mathrm{Im}A_l^I(\nu)=\frac{[\nu/(\nu+1)]^{1/2}}{|A_l^I(\nu)^{-1}|^2}, \quad (10)$$

which corresponds to the assumption of elastic unitarity in the crossed channels. The partial-wave series in Eq. (8) is truncated after p waves. Thus, crossing symmetry is satisfied only approximately.

A word about our approximations is now in order. The threshold for inelastic scattering lies at $\nu=3$ with the production of one pion pair (production of odd numbers of pions is forbidden by G-parity conservation). However, it is believed[5] that inelastic effects are small for $\nu\leq 10$, which corresponds to a total center-of-mass energy of almost 1 BeV. The assumption of elastic unitarity thus gives us the correct right-hand-cut discontinuity for $\nu\leq 10$. For small ν, the contribution to $f(\nu)$ from $\nu'>10$ is less than 10%.

If the right-hand cut is correct for $\nu\leq 10$, then for $\nu>-11$, $\mathrm{Im}A_l^I(\nu<-1)$ is approximate only in the truncation of the partial-wave series after p waves.

[5] G. F. Chew and S. Mandelstam, Phys. Rev. **119**, 467 (1960); Nuovo Cimento **19**, 752 (1961).

This series has been shown to converge for $\nu>-9$,[5,6] but the lowest terms are known to dominate only near $\nu=-1$. For small ν, the contribution to $L_l{}^I(\nu)$ from $\nu'<-9$ is from 10 to 20%, depending on the calculation. It is tempting to consider the possibility of performing further subtractions to speed the convergence of the integrals. Two difficulties are immediately apparent, however. First, further subtractions at the origin would cause the integral over the right-hand cut to diverge. Hence, a different subtraction point would have to be chosen. Second, only one of the parametrizations investigated would have polynomials of high enough order in all waves. We would not be able to investigate the effect of varying the parametrizations, since we are restricted to a total of seven parameters by our formulation.

The invariance of $A(s,t,u)$ under exchange of identical pions results in two fundamental equations.[3,5] The first,

$$A^I(s,t,u)=(-1)^I A^I(s,u,t)\,, \tag{11}$$

is the familiar result of Bose statistics, from which follows the requirement that a Legendre-polynomial expansion of A^I may contain only terms for which $(I+l)$ is even. Since we restrict our considerations to s and p waves, we need to consider only $A_0{}^0$, $A_0{}^2$, and $A_1{}^1$.

The second result of crossing symmetry is

$$A^I(s,t,u)=(-1)^I\sum_{I'}\chi_{II'}A^{I'}(u,t,s)\,, \tag{12}$$

where the matrix χ is given in Eq. (9). Its similarity to the above is apparent when it is written

$$X^I(s,t,u)=(-1)^I X^I(u,t,s)\,, \tag{13}$$

where

$$\begin{aligned} X^0&=A^0+2A^2\,,\\ X^1&=A^0+\tfrac{3}{2}A^1-\tfrac{5}{2}A^2\,,\\ X^2&=A^0-\tfrac{9}{2}A^1-\tfrac{5}{2}A^2\,. \end{aligned} \tag{14}$$

In terms of the t-channel variable $z_t=s-u$,

$$X^I(t,z_t)=(-1)^I X^I(t,-z_t)\,, \tag{15}$$

which, when differentiated variously and evaluated at the symmetry point, yields an infinity of conditions

$$(\partial^m/\partial t^m)(\partial^n/\partial z_t{}^n)X^I(s,t,u)=0\,,\quad (I+n)\text{ odd}. \tag{16}$$

When expressed in terms of the s-channel variables

$$\begin{aligned} s&=-\tfrac{1}{2}(t-4)+\tfrac{1}{2}z_t\,,\\ z_s&=\tfrac{1}{2}(3t-4)+\tfrac{1}{2}z_t\,, \end{aligned} \tag{17}$$

via the chain rule, these yield derivative conditions for the isospin amplitudes $A^I(s,z_s)$. The four third-derivative equations are (note that all functions are evaluated at the symmetry point)

$$\frac{\partial^3A^0}{\partial s^3}+\frac{7}{2}\frac{\partial^3A^2}{\partial s^3}=-7\frac{\partial^3A^0}{\partial s\partial z_s{}^2}-\frac{1}{2}\frac{\partial^3A^2}{\partial s\partial z_s{}^2}\,, \tag{18a}$$

$$\frac{\partial^3A^0}{\partial s^3}-\frac{5}{2}\frac{\partial^3A^2}{\partial s^3}=\frac{27}{2}\frac{\partial^3A^1}{\partial s^2\partial z_s}\,, \tag{18b}$$

$$\frac{\partial^3A^0}{\partial s\partial z_s{}^2}-\frac{5}{2}\frac{\partial^3A^2}{\partial s\partial z_s{}^2}=\frac{3}{2}\frac{\partial^3A^1}{\partial z_s{}^3}\,, \tag{18c}$$

$$\frac{\partial^3A^1}{\partial s^2\partial z_s}=\frac{\partial^3A^1}{\partial z_s{}^3}\,. \tag{18d}$$

To utilize the derivative conditions, we expand the isospin amplitudes in partial waves. This expansion is known to converge inside the Mandelstam triangle. We substitute for s in terms of ν and note that

$$P_l(\cos\theta_s)=P_l(z_s/4\nu)\,. \tag{19}$$

Since $\cos\theta_s$ is a function of ν, when differentiating a partial-wave expansion by ν we find that the lowest-order terms involve only derivatives of the partial-wave amplitudes, while higher-order terms involve the amplitudes as well as their derivatives. Thus, higher partial waves become more important the higher the order of differentiation. We take this into account by including d waves in the second-order equations and both d and f waves in the third-order equations. They are then removed by assuming simple parametrizations for them and combining equations.

We assume that the f-wave amplitude, which we keep in the third-derivative equations, may be parametrized as

$$A_3{}^1(\nu)=K_3{}^1\nu^3\,, \tag{20}$$

thus taking into account the threshold behavior of the amplitude $A_l\propto\nu^l$.

Expanding in partial waves, truncating the series as discussed above, and expressing the derivative equations in terms of ν give the following (again, functions are evaluated at the symmetry point $\nu=-\frac{2}{3}$):

$$2A_0{}^0=5A_0{}^2\,, \tag{21}$$

$$\frac{dA_0{}^0}{d\nu}=-2\frac{dA_0{}^2}{d\nu} \tag{22a}$$

$$=-9A_1{}^1\,, \tag{22b}$$

$$\frac{d^2A_0{}^0}{d\nu^2}-\frac{5}{2}\frac{d^2A_0{}^2}{d\nu^2}-\frac{5}{2}\left(\frac{d^2A_2{}^0}{d\nu^2}-\frac{5}{2}\frac{d^2A_2{}^2}{d\nu^2}\right)=\frac{243}{8}A_1{}^1+\frac{81}{4}\frac{dA_1{}^1}{d\nu}\,, \tag{23a}$$

$$45(A_2{}^0-\tfrac{5}{2}A_2{}^2)=-(27/2)A_1{}^1-9(dA_1{}^1/d\nu)\,, \tag{23b}$$

$$4\left(\frac{d^2A_0{}^0}{d\nu^2}-\frac{d^2A_0{}^2}{d\nu^2}\right)=-135(A_2{}^0-7A_2{}^2)+10\left(\frac{d^2A_2{}^0}{d\nu^2}-\frac{d^2A_2{}^2}{d\nu^2}\right)\,, \tag{23c}$$

[6] H. Lehmann Nuovo Cimento **10**, 579 (1958).

$$\frac{1}{15}\left(\frac{d^3A_0^0}{d\nu^3}+\frac{7}{2}\frac{d^3A_0^2}{d\nu^3}\right)=\frac{1}{6}\left(\frac{d^3A_2^0}{d\nu^3}+\frac{7}{2}\frac{d^3A_2^2}{d\nu^3}\right)$$
$$-\frac{27}{8}(14A_2^0+A_2^2)-\frac{9}{8}\left(14\frac{dA_2^0}{d\nu}+\frac{dA_2^2}{d\nu}\right), \quad (24a)$$

$$\frac{1}{27}\left(\frac{d^3A_0^0}{d\nu^3}-\frac{5}{2}\frac{d^3A_0^2}{d\nu^3}\right)-\frac{5}{54}\left(\frac{d^3A_2^0}{d\nu^3}-\frac{5}{2}\frac{d^3A_2^2}{d\nu^3}\right)$$
$$=-\frac{81}{8}A_1^1-\frac{27}{4}\frac{dA_1^1}{d\nu}-\frac{9}{4}\frac{d^2A_1^1}{d\nu^2}-\frac{21}{2}K_3^1, \quad (24b)$$

$$9(A_2^0-\tfrac{5}{2}A_2^2)+3\left(\frac{dA_2^0}{d\nu}-\frac{5}{2}\frac{dA_2^2}{d\nu}\right)=14K_3^1, \quad (24c)$$

$$\frac{27}{4}A_1^1+\frac{9}{2}\frac{dA_1^1}{d\nu}+\frac{3}{2}\frac{d^2A_1^1}{d\nu^2}=-42K_3^1. \quad (24d)$$

If we represent the d-wave isospin amplitudes by the parametrization

$$A_2^I(\nu)=K_2^I\nu^2, \quad (25)$$

we may combine Eqs. (23a) and (23b) to get

$$\frac{d^2A_0^0}{d\nu^2}-\frac{5}{2}\frac{d^2A_0^2}{d\nu^2}=27A_1^1+18\frac{dA_1^1}{d\nu}. \quad (26)$$

From the six remaining independent equations, we may develop one equation relating the s- and p-wave isospin amplitudes. This is not possible using only the two remaining second-derivative equations if we include a d-wave contribution. Therefore, we must also use the third-derivative equations, including the f-wave contribution parametrized as in Eq. (20). However, if we are to give this much attention to the f wave, we may also improve our parametrization of the d wave. Hence, we now write the d-wave amplitude as

$$A_2^I(\nu)=C_2^I\nu^2+D_2^I\nu^3. \quad (27)$$

Using five of the six equations, we eliminate the five d- and f-wave parameters, arriving at the desired extra equation in s and p waves only:

$$\frac{1}{3}\left(\frac{d^3A_0^0}{d\nu^3}-\frac{5}{2}\frac{d^3A_0^2}{d\nu^3}\right)$$
$$=\frac{675}{8}A_1^1+\frac{225}{4}\frac{dA_1^1}{d\nu}+\frac{75}{4}\frac{d^2A_1^1}{d\nu^2}. \quad (28)$$

[Actually, it is possible to do this using only Eqs. (24b)–(24d), since we need not solve explicitly for the d- and f-wave parameters and can remove them in combination.] Equations (21), (22a) and (22b), (26), and (28) now constitute an independent set which is used in the evaluation of s- and p-wave parameters.

Finally, it is necessary to clarify the reasoning behind the two different d-wave parametrizations used in obtaining Eqs. (26) and (28). Had we represented d waves by Eq. (27) only, the second-derivative equations would not have sufficed to derive an equation, and we would have had to combine them with third-derivative equations to find both equations. It is hoped that the more rapid convergence of the second-order equation is more important than the expanded parametrization.

After the s- and p-wave amplitudes have been determined, to check the validity of the above assumptions, we evaluate the d- and f-wave amplitudes at the symmetry point. For our best solution, the larger d-wave amplitude is less than 2% of the smaller s-wave amplitude and about 40% of the small p-wave amplitude (which is 4% of the s wave). The f-wave amplitude is smaller than the d-wave amplitude by two orders of magnitude. Thus, truncation of the partial-wave series, with higher waves removed from higher-derivative equations, is meaningful. d-wave amplitudes computed from the two parametrizations differ by about 20%. The reasonableness of this result supports the argument for the use of the different d-wave parametrizations.

III. PARAMETRIZATIONS

In Eq. (5) we introduced the functions $P_l^I(\nu)$. Recalling that inelastic effects are neglected in the integrals in Eq. (5), in the hope of getting more information from the symmetry point equations we do not restrict ourselves to polynomial forms of $P_l^I(\nu)$. While our formulation prohibits zeros of $A_l^I(\nu)$ off the real axis, they may occur on it; and since polynomial forms of $P_l^I(\nu)$ do not allow this behavior, it is felt that they are unduly restrictive. Therefore, in four of the five parametrizations investigated, pole terms are explicitly built into one or more of the $P_l^I(\nu)$.

Using Eqs. (21), (22a) and (22b), (26), and (28), plus the mass and width of ρ, we can evaluate seven parameters. In all of the parametrizations seven parameters are used, of which three are in the p wave, and the remaining are shared between the isospin-zero and -two s waves.

Parametrization 1:

$$P_0^{I=0,2}(\nu)=\alpha_{0,2}+\beta_{0,2}\nu,$$
$$P_1^1(\nu)=\alpha_1+\beta_1\nu+\gamma_1\nu^2. \quad (29)$$

Parametrization 2:

$$P_0^{I=0,2}(\nu)=\alpha_{0,2}/(1-\beta_{0,2}\nu),$$
$$P_1^1(\nu)=\alpha_1+\beta_1\nu+\gamma_1\nu^2. \quad (30)$$

Parametrization 3:

$$P_0^0(\nu)=\alpha_0+\beta_0/(1-\gamma_0\nu),$$
$$P_0^2(\nu)=\alpha_2, \quad (31)$$
$$P_1^1(\nu)=\alpha_1+\beta_1\nu+\gamma_1\nu^2.$$

Parametrization 4:

$$P_0^0(\nu)=\alpha_0,$$
$$P_0^2(\nu)=\alpha_2+\beta_2/(1-\gamma_2\nu), \quad (32)$$
$$P_1^1(\nu)=\alpha_1+\beta_1\nu+\gamma_1\nu^2.$$

Parametrization 5:

$$P_0{}^{I=0,2}(\nu)=\alpha_{0,2}+\beta_{0,2}\nu,$$
$$P_1{}^1(\nu)=\alpha_1+\beta_1/(1-\gamma_1\nu). \tag{33}$$

Correct p-wave resonant behavior is enforced by requiring

$$\left(\frac{\nu^3}{\nu+1}\right)^{1/2}\cot\delta_1{}^1\Big|_{\nu_\rho}=0 \tag{34}$$

and

$$\frac{d}{d\nu}\left[\left(\frac{\nu^3}{\nu+1}\right)^{1/2}\cot\delta_1{}^1\Big|_{\nu_\rho}\right]=-\frac{1}{\gamma}\left(\frac{\nu_\rho{}^3}{\nu_\rho+1}\right)^{1/2}. \tag{35}$$

(We use $\nu_\rho=6.25$ corresponding to $m_\rho=753$ MeV, $m_\pi=140$ MeV.) Thus, at the ρ resonance the p wave has the same slope as if it were given by the Breit-Wigner form

$$A_1{}^1(\nu)=\left(\frac{\nu+1}{\nu}\right)^{1/2}\frac{\gamma}{\nu_\rho-\nu-i\gamma} \tag{36}$$

(corresponding to a ρ width of 110 MeV, $\gamma=1.15$).

Here we have two conditions involving only p-wave parameters. By arbitrarily specifying any of the p-wave parameters, we may completely specify the p wave, greatly simplifying computation of the s-wave parameters. (Of course this leaves one of the crossing equations unused.) In each iterative calculation, α_1 is arbitrarily fixed. After iteration is complete, the unused crossing equation is plotted as a function of α_1, yielding solutions satisfying all crossing equations.

We solve for the s-wave parameters as follows. Equations (21), (22a) and (22b), (26), and (28) are written in terms of the inverse amplitudes, and derivatives are taken. [Derivatives of $L_l{}^I(\nu)$ are found by differentiating Eq. (7) and evaluating the resulting integrals. These integrals generally converge faster than those for $L_l{}^I(\nu)$.] Four of the resulting nonlinear algebraic equations are combined, yielding a single equation in one of the inverse amplitudes. This equation is of third order for parametrizations 1 and 5, fourth order for parametrization 2, and sixth order for parametrizations 3 and 4. Its order depends upon both the parametrization and the equations from which it is developed. To keep the order low, the obvious equation to plot is Eq. (28). However, when initial calculations were made for parametrization 3, no real roots were found. We therefore decided arbitrarily to plot Eq. (26a) for parametrization 3 and Eq. (26b) for parametrization 4.

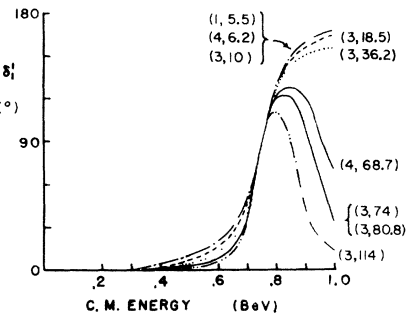

FIG. 1. p-wave phase shifts. For solution (3, 36.2), $\delta_1{}^1$ returns through 90° above 2 BeV.

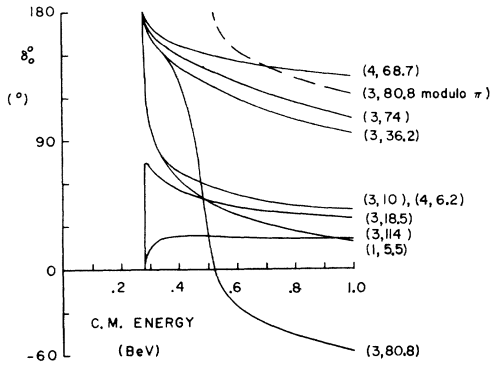

FIG. 2. s-wave $I=0$ phase shifts.

Iteration is begun by neglecting $L_l{}^I(\nu)$ and its derivatives and by computing parameters. During iteration the real root closest to that preceding is chosen, and a unique set of parameters is computed from it. When iteration converges, we associate the result with the initial root from which it developed. This orders the results unambiguously for plotting.

Numerical integrations are performed using Simpson's rule. First, the variables $z=(-\nu)^{-1/2}$ for $\nu<-1$, and $z=(\gamma+1)^{-1/2}$ for $\nu>0$ are introduced, which map the regions of integration between 1 and 0.

TABLE I. Scattering lengths; coupling constant.

Solution	$\mu a_0{}^0$	$\mu a_0{}^2$	$\mu^3 a_1{}^1$	λ
(1, 5.5)	−4.6	2.9	0.18	−0.93
(4, 6.2)	−5.7	1.3	0.16	−0.63
(3, 10) [a]	−25±15	0.95±0.15	0.10	−0.46
(3, 18.5)	38	1.1	0.054	−0.41
(3, 36.2) [a]	−0.69±0.04	−0.37±0.03	0.028	0.19
(4, 68.7)	−0.46	−0.22	0.015	0.12
(3, 74)	−0.57	−0.29	0.014	0.15
(3, 80.8)	−0.70	−0.35	0.012	0.20
(3, 114)	0.85	0.26	0.0088	−0.12

[a] See Ref. 7.

[7] It was not possible to satisfy the plotted crossing condition to arbitrary accuracy, since the effects of small changes of α_1 were often overwhelmed by larger iteration effects. In all solutions but (3, 10) and (3, 36.2), the plotted equation is satisfied within 3%. In solution (3, 36.2), bounding solutions are both within 22% of satisfying the plotted condition, and in (3, 10) they are within 16 and 36%. Nevertheless, phase shifts are well determined, differing only in the s waves. For solution (3, 10) above 350 MeV, uncertainties are ±1° for $I=0$ and ±2° for $I=2$. For solution (3, 36.2), uncertainties grow smoothly from threshold to ±3° for $I=0$ and ±4° for $I=2$ at the ρ mass.

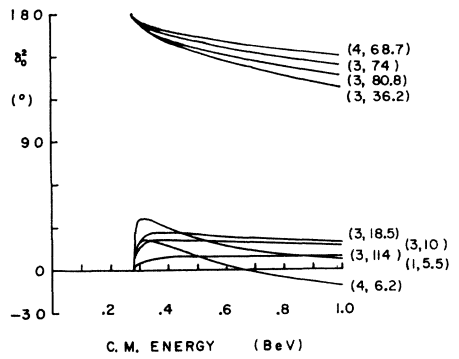

FIG. 3. s-wave $I=2$ phase shifts.

A grid is then chosen by dividing this unit interval into equal parts. Since it is very fine near the origin in ν, and becomes increasingly coarse with increasing $|\nu|$, this further weights the better known region of small $|\nu|$.

Since we cannot calculate points at infinity, the integrals are cut off two grid spaces short. The grid was set at 90 intervals in all calculations. Tightening it to 120 intervals changed the most sensitive parameter by 3% in a typical calculation. The cutoff at $\nu=-2025$ was far beyond the point where the integrand became negligible.

IV. RESULTS

Calculations were carried out for positive values of α_1 between 1 and 200. Nine solutions were found for parametrizations 1, 3, and 4. It is convenient to label these solutions by the parametrization to which they belong and the value of α_1 for which they occur. Thus (1, 5.5) denotes the solution for parametrization 1 with $\alpha_1=5.5$. Phase shifts for the nine solutions are plotted in Figs. 1, 2, and 3.[7]

The p-wave phase shifts are seen to be neatly ordered by their α_1 values. This is because for all of our solutions the p wave is given by

$$(\nu^3/\nu+1)^{1/2}\cot\delta_1{}^1=\alpha_1+\beta_1\nu+\gamma_1\nu^2+\nu f(\nu)+L_1{}^1(\nu)\,, \quad (37)$$

which is required to vanish with fixed slope at ν_ρ. The integral contributions do not vary more rapidly than ν^2, so that this function is roughly parabolic, and we find correlation between threshold values and high-energy behavior. The value of α_1 corresponding to a straight line fitting our resonance conditions is 32, which separates the calculated phase shifts which return through 90° from those which do not.

TABLE II. Positions of poles of $A_0{}^0(\nu)$. The resonance pole may be compared with the Breit-Wigner prediction of $6.25-1.15i$.

Solution	Resonance pole	Physical-sheet pole
(4, 68.7)	$6.0-1.00i$	$11.4+1.8i$
(3, 74)	$5.8-0.95i$	$10.1+1.4i$
(3, 80.8)	$5.9-0.94i$	$9.9+1.7i$
(3, 114)	$5.9-0.87i$	$8.5+1.1i$

TABLE III. Maximum $\nu<-1$ for agreement of left-hand cut calculated from crossing and from A^{-1}.

Solution	$\mathrm{Im}A_1{}^1$	$\mathrm{Im}A_0{}^0$	$\mathrm{Im}A_0{}^2$
(1, 5.5)	−5.6	−9.0	−4.2
(4, 6.2)	−5.6	−5.9	−9.0
(3, 10)	−1.0	−1.1	−1.2
(3, 18.5)	−1.0	−1.9	−1.5
(3, 36.2)	−5.1	−12.0	−9.0
(4, 68.7)	−5.1	−7.4	−12.0
(3, 74)	−1.8	−7.0	−11.0
(3, 80.8)	−1.2	−8.4	−9.6
(3, 114)	−1.1	−6.6	−4.4

In Table I, scattering lengths are listed along with values of the Chew-Mandelstam coupling constant $\lambda=-\frac{1}{5}A_0{}^0(\nu=-\frac{2}{3})$. Comparing this table with Table I of Kang[3] yields some striking similarities. For $\lambda<-0.4$, we see that the $I=0$ s waves develop bound states. For $\lambda=-0.1$, s-wave scattering lengths agree within 25%, and both s-wave phase shifts are within 2% at the ρ mass. For $0.1<\lambda<0.2$, our s-wave scattering lengths are neatly bounded by Kang's ($0.4<-\mu a_0{}^0<0.7$ and $0.2<\mu a0^2<0.4$), and our phase shifts for all solutions but (3, 80.8) are similar above threshold. Thus, our results are consistent with earlier work using a similar formulation.

It is interesting that our completely determined formalism yields such a wide spectrum of solutions. This multiplicity, of course, stems from the multiple roots of our symmetry-point equations, and is the price which we must pay for our expanded parametrizations. We must further investigate our solutions to determine their physical acceptability.

$A_l{}^I(\nu)$ must have no poles on the nearby physical sheet, a condition which is violated by all but one solution. On the real axis between $\nu=-1$ and 0, $A_l{}^I(\nu)$ is real. In this region $(A_0{}^0)^{-1}$ vanishes for solutions (1, 5.5), (3, 10) (4, 6.2), and (3, 18.5), and $(A_0{}^2)^{-1}$ vanishes for solution (4, 68.7). Hence, these solutions must be regarded as physically unacceptable.[8]

The fall of $\delta_1{}^1$ through 90° is associated with a pole of $A_1{}^1(\nu)$ on the nearby physical sheet for solutions (4, 68.7), (3, 74), (3, 80.8), and (3, 114). This is determined by analytically continuing $F_1{}^1(\nu)$. By fitting straight lines to the integral contributions and to the imaginary part (all excellent approximations for $\nu>2$), and then continuing above the real axis, well-defined zeros of $F_1{}^1(\nu)$ are found. By continuing below the real axis, the unphysical sheet poles associated with the ρ resonance are similarly found. In Table II, the positions of these poles are listed. The physical sheet poles are indeed near the real axis, and the unphysical sheet poles

[8] From the signs of the residues, solutions (3, 18.5) and (4, 68.7) have ghost poles, while the others have bound-state poles. The ghosts are in the immediate vicinity of poles of $A_l{}^{I-1}$, and these solutions are the only ones with poles of $A_l{}^{I-1}$ in this region.

compare favorably with the prediction of the Breit-Wigner form of Eq. (36). If we apply this analysis to solution (3, 36.2), whose p-wave phase shift falls through 90° above 2 BeV, we find a pole at $\nu=50+10i$. This is so far away that we consider it irrelevant.

The status of solutions with physical sheet poles in the p wave is unclear. Ideally, we should throw them out as unphysical. However, as only one of the p-wave parameters is fixed by crossing symmetry, this may be uncalled for. While their p-wave phase shifts are unexpected, the problems occur above the ρ mass, and it might be argued that their effects on the s waves are unimportant. However, we may use another argument to discriminate against them.

As we have mentioned, $\mathrm{Im}A_l^I$ for $\nu<-1$ is given only approximately by the crossing equation (8). For each of our solutions, we have computed this quantity from $(A_l^I)^{-1}$ and have compared it with the value of the crossing integral. In all cases agreement is excellent (better than 5%) out to a point where the values diverge rapidly. These points are listed in Table III. For the solutions lacking poles below threshold, we see that the s-wave argeement extends much farther than has been reported previously.[3,4] However, the p waves agree extensively only for solution (3, 36.2). Because the s waves have been shown to contribute strongly to the p wave,[3] this solution is preferable to the others. The left-hand cuts for this solution are plotted in Fig. 4.

Thus, of the solutions lacking poles of the s-wave amplitude below threshold, only (3, 36.2) lacks nearby physical sheet poles of the p wave and is self-consistent in all partial waves over an appreciable region of the left-hand cut. It is unquestionably our "best" solution.

Finally, we note that solution (3, 80.8) has a physical sheet pole in A_0^0 at $\nu=1.75+0.26i$. It corresponds to the rapid phase-shift drop through 90° at $\nu=1.65$, and was found by fitting a parabola to $\mathrm{Re}F_0^0(\nu)$ in this region and continuing above the real axis. As this physical sheet pole is near the real axis, this solution is unacceptable.

Experimental phase shifts for comparison with our results are not well determined. Below 600 MeV, as

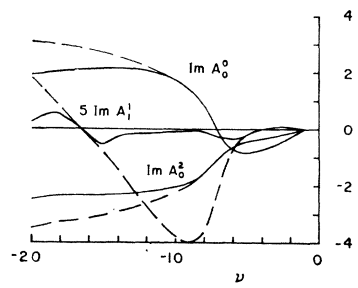

FIG. 4. Left-hand cuts for solution (3, 36.2). Solid curves are from the inverse amplitudes, and dashed curves are from the crossing integrals.

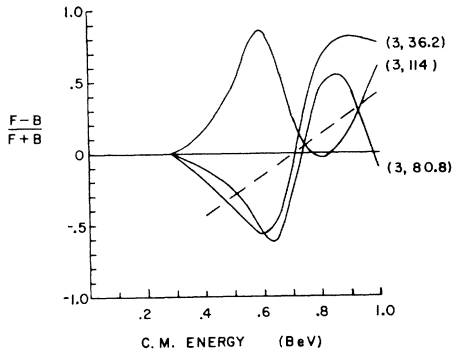

FIG. 5. Forward-backward asymmetry for $\pi^-\text{-}\pi^0$ scattering for three of our solutions. The dashed curve is a hand-drawn fit to the experimental points of Ref. 10.

discussed by Bander, Shaw, and Fulco,[9] sufficiently accurate data for reliable determination of the $\delta_0{}^I$ are not available from $\pi N\rightarrow\pi\pi N$ reactions. This is because the s-wave phase shifts depend critically on $\delta_1{}^1$, which is accurately known only near the ρ. Because of the asymmetry of $\pi^-\text{-}\pi^0$ scattering (to which only $A_0{}^2$ and $A_1{}^1$ contribute), $\delta_0{}^2$ is believed to be small and negative. In Fig. 5, this asymmetry is plotted for three of our solutions. Those with negative $\delta_0{}^2$ agree qualitatively with the experimental curve from Ref. 10.

Phase-shift analyses performed on compilations of data by Walker *et al.*[11] and by Malamud and Schlein[12] yield qualitatively similar results for $\delta_0{}^0$ in the 600–900-MeV range—solutions climbing steeply through 90° and solutions slowly increasing in the 70–90° range. Walker *et al.* favor the nonresonant result, while Malamud and Schlein prefer a resonant solution which is not amenable to a Breit-Wigner fit. However, the latter authors refuse to rule out the nonresonant solution.

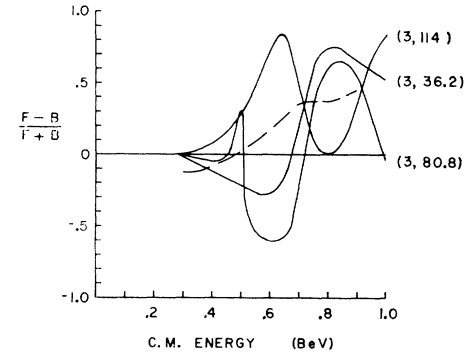

FIG. 6. Forward-backward asymmetry for $\pi^+\text{-}\pi^-$ scattering for three of our solutions. The dashed curve is a hand-drawn fit to the experimental histogram of Ref. 13.

[9] M. Bander, G. L. Shaw, and J. R. Fulco, Phys. Rev. **168**, 1679 (1968).

[10] D. H. Miller, L. Gutay, P. B. Johnson, F. J. Loeffler, R. L. McIlwain, R. J. Sprafka, and R. B. Willman, Phys. Rev. **153**, 1423 (1967).

[11] W. D. Walker, J. Carroll, A. Garfinkel, and B. Y. Oh, Phys. Rev. Letters **18**, 630 (1967).

The forward asymmetry of π^+-π^- scattering near the ρ mass is more firmly established. Jones *et al.*[13] have investigated this asymmetry extensively at lower energies and find that below 500 MeV it changes sign. They conclude that their results are consistent with a negative δ_0^0 falling smoothly from threshold. In Fig. 6, this asymmetry is plotted for three of our results, along with the experimental curve of Ref. 13. In order for solution (3, 36.2) to agree qualitatively with experiment, δ_0^0 would have to decrease somewhat faster, passing through 90° near or somewhat below the ρ mass, as conjectured by Chew.[14] (This would also bring it into qualitative agreement with the nonresonant solutions above.) In addition, it would increase δ_0^2-δ_0^0 from its present value of 23° at the mass of the K meson, bringing it into better agreement with the value of 57° reported by Bennett *et al.*[15] To see if such a solution was obtainable, solution (3, 36.2) was reinvestigated, using a ρ width of 160 MeV. However, this solution proved to be quite stable under variation of this parameter.

We must conclude that our best solution (3, 36.2) is not in close agreement with experiment. However, we feel that a physically acceptable solution of this type may yet be obtained from this formalism in better agreement with experiment. In search of such a solution, the difficulties due to the p-wave phase shifts should be removed. Further, it may be necessary to include higher partial waves or even to abandon the assumption of elastic unitarity. However, it seems reasonable that some relatively minor changes in the formulation might lead to a solution with δ_0^0 intermediate between those of (3, 36.2) and (3, 10), and with negative δ_0^2, which would be in good agreement with experiment.

[12] E. Malamud and P. E. Schlein, Phys. Rev. Letters **19**, 1056 (1967).

[13] L. W. Jones, E. Bleuler, D. O. Caldwell, B. Elsner, D. Harting, W. C. Middelkoop, and B. Zacharov, Phys. Rev. **166**, 1405 (1968).

[14] G. F. Chew, Phys. Rev. Letters **16**, 60 (1966).

[15] S. Bennett, D. Nygren, H. Saal, J. Steinberger, and J. Sunderland, Phys. Rev. Letters **19**, 997 (1967).

ACKNOWLEDGMENTS

The author wishes to thank Professor M. H. Ross for suggesting the problem and for his encouragement and guidance during its solution. Thanks are also extended to Professor G. Kane for many enlightening discussions and to Professor K. Kang for a computer program from which the author's was developed.

PHYSICAL REVIEW VOLUME 183, NUMBER 5 25 JULY 1969

Exchange Degeneracy and the Pomeranchukon*

R. H. GRAHAM AND R. K. LOGAN
Department of Physics, University of Toronto, Toronto, Canada
(Received 7 March 1969)

We show that if exchange degeneracy is valid, the Pomeranchukon is not a Regge trajectory.

THE unique nature of the Pomeranchuk trajectory became evident from the very beginning of Regge phenomonology. It dominates all the other trajectories and has an intercept $\alpha(0)$ equal to 1. The closest competitors, the P', ω, and ρ, have intercepts near 0.5. All the normal trajectories have slopes $\alpha'(0)$ approximately equal to 1 GeV^{-2}. The P, on the other hand, must have $\alpha'(0) \leq 0.30$ [1] to fit the nonshrinkage of the πp differential cross section. All the trajectories have particles associated with them; the P' has the f_0, the R has the A_2, the ρ has the ρ, etc., with the sole exception of the Pomeranchukon. Many trajectories seem to possess exchange-degenerate partners, with the notable exception of the P. By applying the concept of exchange degeneracy to KK and pp elastic scattering, we shall show that this absence indicates that the Pomeranchukon is not a normal Regge trajectory. This lends support to the notion that the Pomeranchukon is a diffractive effect,[2,3] and not a trajectory.

Let us begin our investigation by assuming that the Pomeranchukon corresponds to a Regge trajectory. If a trajectory lies in the s channel, then it arises from the potential due to the exchanges in t and u channels. Let us consider the P trajectory as arising from $K^+ + K^-$ elastic scattering (see Fig. 1). The t channel corresponds

* Supported in part by the National Research Council of Canada.

[1] W. Rarita *et al.*, Phys. Rev. **165**, 1615 (1968).

[2] T. T. Wu and C. N. Yang, Phys. Rev. **137**, B708 (1965); T. T. Chou and C. N. Yang, *ibid.* **175**, 1832 (1968); H. D. I. Abarbanel, S. D. Drell, and F. J. Gilman, Phys. Rev. Letters **20**, 280 (1968); L. Durand and R. Lipes, *ibid.* **20**, 637 (1968); R. C. Arnold and S. Fenster, in Proceedings of the 1968 Topical Conference on High-Energy Hadron Reactions, CERN, 1968 (unpublished); C. B. Chiu and J. Finkelstein, Nouvo Cimento **47A**, 649 (1968).

[3] F. Henyey, G. L. Kane, J. Pumplin, and M. Ross, Phys. Rev. Letters **21**, 946 (1968); R. C. Arnold and M. L. Blackmon, Phys. Rev. **176**, 2082 (1968).